An improved *p* chart for monitoring high quality processes based on Cornish-Fisher quantile correction

Silvia Joekes [1] and Emanuel Pimentel Barbosa [2]

1 Instituto de Estadística, Universidad Nacional de Córdoba, Córdoba, CP 5000, Argentina.

2 Dpto. Estatística, Imecc/UNICAMP, Barao Geraldo 13083-859, Campinas-SP, Brazil.

Abstract

The conventional Shewhart 3-sigma *p* control chart constructed by the normal approximation for the binomial data suffers a serious inaccuracy in the modeling process and control limits specification when the true rate of nonconforming items is small. We offer an improved *p* chart which can provide a large improvement over the usual *p* chart for attributes. This new chart, based on the Cornish-Fisher expansion, is corrected to order $n^{-3/2}$, where n is the sample size of inspections units. This chart is also better than the modified *p* chart corrected only to order n^{-1}, especially in the sense that it allows monitoring lower values of *p*. We compare our improved *p* chart with both and show the benefits of including a new term of correction in the Cornish-Fisher expansion of quantiles for monitoring high-quality processes.

Key Words: Attribute control charts, False alarm risk, Nonconforming proportion, Statistical quality control

1. Introduction

When Shewhart (1926) developed the control charts for proportion of nonconforming items, probably he never thought that this proportion could take very small values. In the present, the situation of low nonconforming levels in processes often exists, and the performance of classical attribute control charts becomes inadequate. Historically, these charts have been developed by using the normal approximation to the binomial distribution to the sample statistic, but it is far from adequate for the situation of low defect level and when the sample size is not large enough, mainly due to skewness in the exact distribution. For small *p* values, the binomial distribution is highly asymmetric, and as a result, any attempt to monitor *p* with symmetric control limits, is subject to making more false alarm in detecting an increase or a decrease in *p* than claimed.

In order to improve *p* charts for a low-nonconformity and high-yield process many authors have proposed alternative methods that have been extensively studied in the literature (see Chen, 1998; Goh and Xie, 1995; Kuralmani et al., 2002; Xie; Wang, 2009 and Goh, 1993). A good survey for the control charts of high-quality processes can be found in Xie et al. (2002). Although these proposed charts can increase the monitor accuracy, they still lack achievement of desirable accuracy when the true *p* is very small and *n* is not large. Some other modifications can be found in Quesenberry (1997), Ryan and Schwertman (1997) and Acosta-Mejia (1999), among others.

Chan et al. (2002) proposed a chart based on the count of consecutive conforming (CCC chart) as well as the cumulative quantity control (CQC) chart, to overcome the difficulty of the poor performance when the defect rate of the process is low. The use of a CCC type control chart has been further studied by Xie and Goh (1993), Ermer (1995), Wu et al. (2000). This chart is very useful for one-at-a-time inspections or tests which are common in automated manufacturing processes. But, the information of the number of items inspected until a defective item is observed, primarily needed for this chart, is different from the information of the proportion of the nonconforming items to all items used for the other charts, as is the case of the *p* chart.

Winterbottom (1993) achieved an improvement in the accuracy probability of the control limits by simple adjustments (3^{rd}order cumulants) derived from the Cornish-Fisher expansion of quantiles to correct non-normalities. He also pointed out that the adjustments are better than normalizing transformations in that the original scale of the data is retained. Winterbottom carried out such a study for attribute charts using the first adjustment in a Cornish-Fisher asymptotic expansion that corrects both bias and skewness. Chen (1998) considered Winterbottom's result for the *p* known case and presented an extension to the *p* unknown case.

The proposal we present here is a new modified *p* chart (based on the Cornish-Fisher expansion) with cumulants until 4^{th} order that allows monitoring processes with very low rate of non-conformities

The paper is organized as follow. The sample nonconforming proportion statistic with its moments formulae and the standard normal-based *p* control chart with its limits and false alarm risk are reviewed in section 2. The *p* control chart based on the Cornish-Fisher expansion with one term of correction and a new improved *p* chart including terms of order $n^{-3/2}$ is presented in section 3. A false alarm comparative study to show the advantages of the new chart in relation to the traditional and modified *p* chart proposed by Winterbottom is presented in section 4. The proposed new chart is illustrated with a numerical example of application with real data in section 5. Final comments and conclusions are presented in section 6, followed by the references.

2. The Normal-based *p* Chart

2.1 The sample nonconforming proportion $\hat{p}$ and its basic properties

(i) **Notation and distribution**: Let X be a discrete random variable denoting the number of trials that result in an outcome of interest, with a binomial distribution of parameters *n* and *p*, where *n* is the number of trials.

If we obtain X successes (nonconforming) in n trials, then the sample proportions denoted by $\hat{p}$, is defined as $\hat{p} = X/n$ (relative binomial). Then, the mean, variance and standard deviation of the sample proportion $\hat{p}$ are, respectively;

$$\mu_p = \mathbb{E}(\hat{p}) = p \quad , \quad \sigma^2 = \mathbb{V}(\hat{p}) = p(1-p)/n \quad , \quad \sigma = \sqrt{p(1-p)/n}$$

(*ii*) Moments (ordinary and central): From the moment generating function of the binomial distribution, ordinary moments are obtained as $\mu'_h = \mathbb{E}(X^h) = M^{(h)}(0)$, where:

$$M_x(t) = \sum_{k=0}^{n} e^{tk}\, p_k = (pe^t + 1 - p)^n$$

with $\quad p_k = \binom{n}{k} p^k (1-p)^{n-k}$, $\quad k = 0,1,2,\ldots, n$

In particular, the first four ordinary moments are given by

$\mu'_1 = \mathbb{E}(X) = np$

$\mu'_2 = \mathbb{E}(X^2) = n^2\, p^2 + np(1-p)$

$$\mu_3' = \mathbb{E}(X^3) = np(1-p)(1-2p) + 3\,n^2p^2(1-p) + n^3p^3$$

$$\mu_4' = \mathbb{E}(X^4) = np(1-p)[1-6p(1-p)] + 6\,n^2p^2(1-p)[(1-2p)+np] + \\ + n^2p^2(1-p^2+n^2p^2)$$

And the central moments are given by

$$\mu_h = E(X-\mu)^h = \sum_{r=0}^{h} \mu_r' \binom{h}{r} (-\mu)^{h-r} \qquad h = 1, 2, \ldots..$$

$$\mu = \mu_1' = \mathbb{E}(X) = np$$

$$\mu_2 = \mu_2' - \mu_1'^2 = \mathbb{V}(X) = np(1-p)$$

$$\mu_3 = \mu_3' - 3\mu_2'\mu_1' + 2\mu_1'^3 = np(1-p)(1-2p)$$

$$\mu_4 = \mu_4' - 4\mu_1'\mu_3' + 6\mu_2'\mu_1'^2 - 3\mu_1'^4 = np(1-p)[1-6p(1-p)] + 3n^2p^2(1-p)^2$$

(***iii***) **Cumulants:** From the Cumulants Generating Function (logarithm of the moments generating function), with the central moments previously standardized, we obtain:

$$K_1 = \mu^* = \frac{\mu}{\sigma}, \quad K_2 = \mu_2^* = \frac{\mu_2}{\sigma^2}, \quad K_3 = \mu_3^* = \frac{\mu_3}{\sigma_3}, \quad K_4 = \mu_4^* - 3\mu_2^{*2} = \frac{\mu_4}{\sigma_4} - 3\left(\frac{\mu_2}{\sigma^2}\right)^2$$

where $\sigma = \sqrt{\mu_2}$

2.2 Normal *p* Control Chart: Limits and False Alarm Risk

(***i***) **Limits***:* The standard 3σ framework calls for limits placed at $\mu_{\hat{p}} \pm 3\hat{\sigma}_{\hat{p}}$. If the true proportions nonconforming p is known or is accurately estimated then the 3σ control chart model gives:

$$\text{UCL} = p + 3\sqrt{\frac{p(1-p)}{n}}, \qquad \text{CL} = p\,, \qquad \text{LCL} = p - 3\sqrt{\frac{p(1-p)}{n}}$$

This approximation is considered good when $np(1-p) > 5$ and $0.1 < p < 0.9$, or when $np(1-p) > 25$, (Xie, 2002).

(***ii***) **False alarm α risk:** The evaluation of a p chart performance can be based on the type I error, which is the probability that $\hat{p}$ does not fall between the upper and the lower limits of the chart (when the process is under control), called false alarm probability.

From the distribution of $\hat{p}$ (relative binomial) under H_0: $p = p_0$, the reference value for α is the usual 0.0027, which is pre-fixed. However, the actual α risk, is given by:

$$\alpha \text{ risk} = \text{P}(\textit{Reject } H_0 |\ H_0 \textit{ is true}) = 1 - [F_X(nUCL) - F_X(nLCL)] =$$

$$= 1 - [\ Pr_{po}(X \leq n\text{UCL}) - Pr_{po}(X \leq n\text{LCL})]$$

as it is usually obtained, with Pr calculated by the binomial distribution

3. The Cornish-Fisher corrected *p* control chart

3.1 The *p* chart with one adjustment

(*i*) Control Limits: Let X be a binomial random variable with sample size n and parameter p. Then $Y = X/n$ is a binomial proportion with $\mu = E(Y) = p$, and central moments of Y, $\mu_2 = V(Y) = p\,(1-p)/n$, $\mu_3 = p(1-p)(1-2p)/n^2$ (using information from the section 2.1). If z_α denote the α quantile of the standard normal distribution then, the αth quantile of Y, denoted by Y_α (named here $Y_\alpha(1)$), is obtained from the Cornish-Fisher expansion with only one correction term (Cornish & Fisher, 1960; Lee & Lee, 1992) as:

$$\frac{Y_\alpha(1) - p}{\sqrt{\frac{p(1-p)}{n}}} \cong z_\alpha + \frac{(z_\alpha^2 - 1)}{6} K_3$$ where K_3 is given in section 2.1 (*iii*))

It follows immediately that:

$$Y_\alpha(1) = p + z_\alpha [p(1-p)/n]^{1/2} + \frac{(z_\alpha^2 - 1)}{6n}(1-2p)$$

Setting $z_\alpha = \pm 3$ gives the improved control limits for *p*-chart as

$$\mathrm{UCL}_1 = p + 3\,[p(1-p)/n]^{1/2} + \frac{4}{3n}(1-2p) = \mathrm{UCL} + \frac{4}{3n}(1-2p)$$

$$\mathrm{LCL}_1 = p - 3\,[p(1-p)/n]^{1/2} + \frac{4}{3n}(1-2p) = \mathrm{UCL} + \frac{4}{3n}(1-2p)$$

Where UCL_1 and LCL_1 are the improved limits with one correction term.

(*ii*) False Alarm Study: The ideal *p* chart, taken as reference, has α risk = α_0, the pre-fixed risk of type-I error (reject H_0 when H_0 is true), that is considered as the usual 0.0027.

The comparison results are presented graphically as a function of the p parameter for a given sample size *n*, for two sided charts (usual α risk and upper α risk). As an example we show the comparative false alarm risk for *n* = 20 (Fig. 1).

[References for the two graphics below are: • Normal approx.; ▲ Cornish-Fisher pre-fixed α_0 = 0.0027]

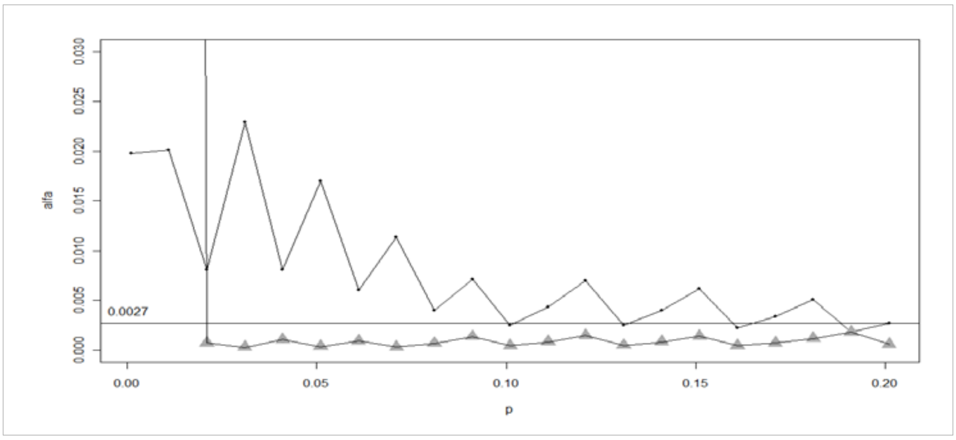

Figure 1: α risk (two sided) of approximated normal versus Cornish-Fisher (one adjustment).

From the figure above, it is clear that the corrected chart presents false alarm risk closer to the reference risk (α_0= 0.0027) than the traditional normal-based chart. However, this correction cannot be used for any value of *p*, only for *p* values greater than 0.02, approximately, when *n* = 20.

If we now consider only the upper risk (probability of crossing the upper limit when H_0 is true), the comparative results are even stronger, in favor of the corrected chart, as show in Figure 2 below.

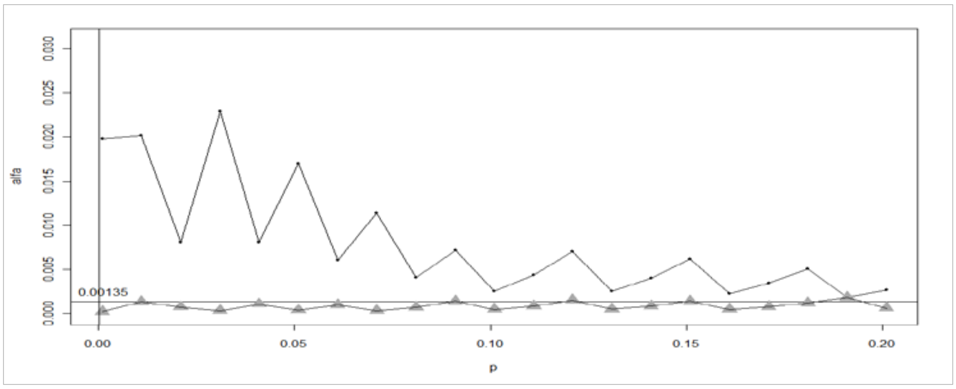

Figure 2: Upper α risk of approximated normal versus Cornish-Fisher (one adjustment)

From the figures above we can see that the correction produced a reduction in the excess of false alarm.

3.2 The *p* chart with two adjustments

***(i)* Control Limits:** Now, we extend further results by Winterbottom (1993) by including new terms of order $n^{-3/2}$ in an improved *p* chart.

By using the Cornish-Fisher expansion of quantiles to obtain a better approximation for the Binomial distribution we correct its non-normality (skewness and kurtosis) using the information from the 3^{rd} and 4^{th} order cumulants (K_3 and K_4).

In this case we add to the information given in section 3.1 (*i*) the fourth-order central moment of *Y*, $\mu_4 = \{np(1-p)[1-6p(1-p)] + 3n^2p^2(1-p)^2\}/n^4$

$$\frac{Y_\alpha(2) - p}{\sqrt{\frac{p(1-p)}{n}}} = z_\alpha + \frac{(z_\alpha^2 - 1)}{6} K_3 + \frac{(z_\alpha^3 - 3z_\alpha)}{24} K_4 - \frac{(2z_\alpha^3 - 5z_\alpha)}{36} K_3^2$$

(where K_3 and K_4 are given in section 2.1 (*iii*), and $Y_\alpha(2)$ is the α-th quantile of *Y* for two adjustments)

Its follows immediately that:

$$Y_\alpha(2) = Y_\alpha(1) + \frac{(z_\alpha^3 - 3z_\alpha)}{24n^2} \frac{[1 - 6p(1-p)]}{[p(1-p)/n]^{1/2}} - \frac{(2z_\alpha^3 - 5z_\alpha)}{36n^2} \frac{(1-2p)^2}{[p(1-p)/n]^{1/2}}$$

Setting $z_\alpha = \pm 3$ gives the improved control limits for p-chart as

$$\mathrm{UCL}_2 = \mathrm{UCL}_1 - \frac{[p(1-p)+2]}{6n^2\,[p(1-p)/n]^{1/2}}$$

$$\mathrm{LCL}_2 = \mathrm{LCL}_1 - \frac{[p(1-p)+2]}{6n^2\,[p(1-p)/n]^{1/2}}$$

Where UCL_2 and LCL_2 are the improved limits with two correction terms.

***(ii)* False Alarm Comparative Study:** Returning to the example of the previous subsection, we show the comparative false alarm risk for n = 20 (Fig. 3).

[References for the two graphics below are: • Normal approx.; ● Cornish-Fisher; pre-fixed α_0= 0.0027]

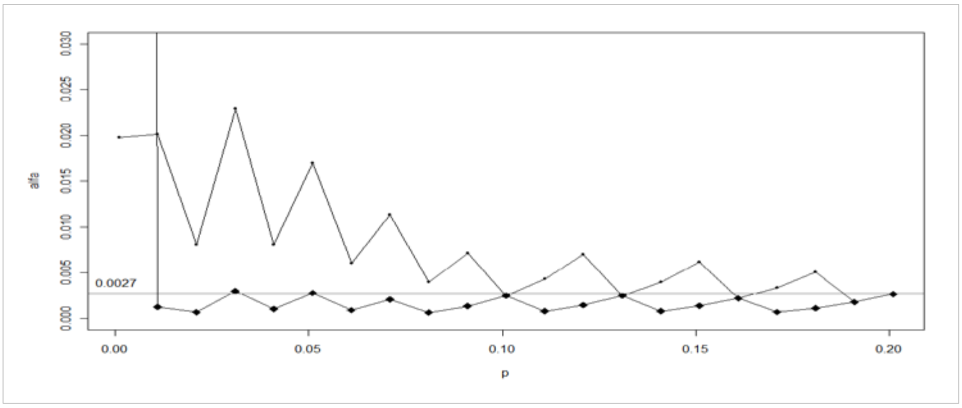

Figure 3: α risk (two sided) of approximated normal versus Cornish–Fisher (two adjustments)

From the figure above, it is clear that the correction (two terms) shows false alarm risk much closer to the reference risk (α_0= 0.0027) than the traditional normal-based chart. Notice also that it allows working with smaller p values than the modified p chart with only one term of correction. However, this correction can be used only for p values greater than 0.01, approximately, when n = 20 (less restrictive than the previous one)

If we now consider only the upper risk, the comparative results are similar to previous (3.2 (*ii*)), as shown in Figure 4 below.

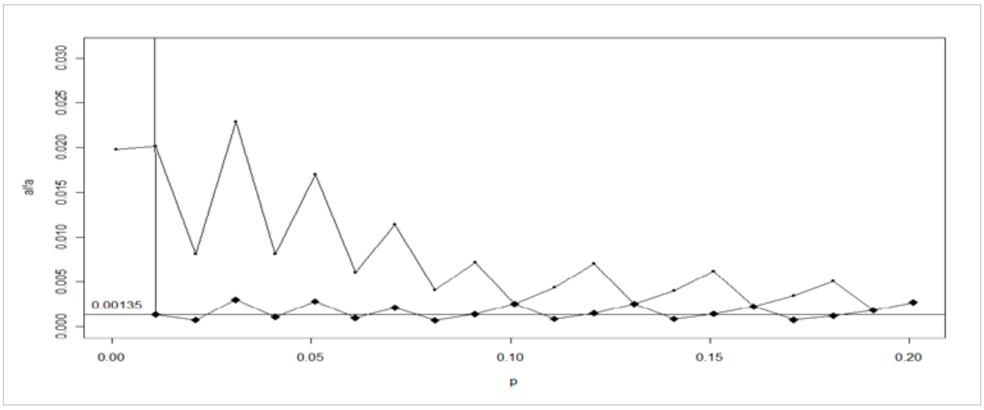

Figure 4: Upper α risk of approximated normal versus Cornish– Fisher (two adjustments)

From the figure above, comparing it with Fig.3, it is clear that the improvement in the *p*-chart is grater in terms of upper α risk than the usual.

4. False Alarm Study for small *n* and *p*

We present graphically the risk of false alarm for three different values of *n*, 20, 10 and 5. In order to show in more detail the comparison between the two charts (corrected with one term and corrected with two terms) for small values of *p*, we present a graph and focused on the values of *p* located in the vicinity of 0.

[References for the three graphics below are: ▲ Cornish-Fisher (one term), ● Cornish-Fisher (two terms); pre-fixed α_0 = 0.0027]

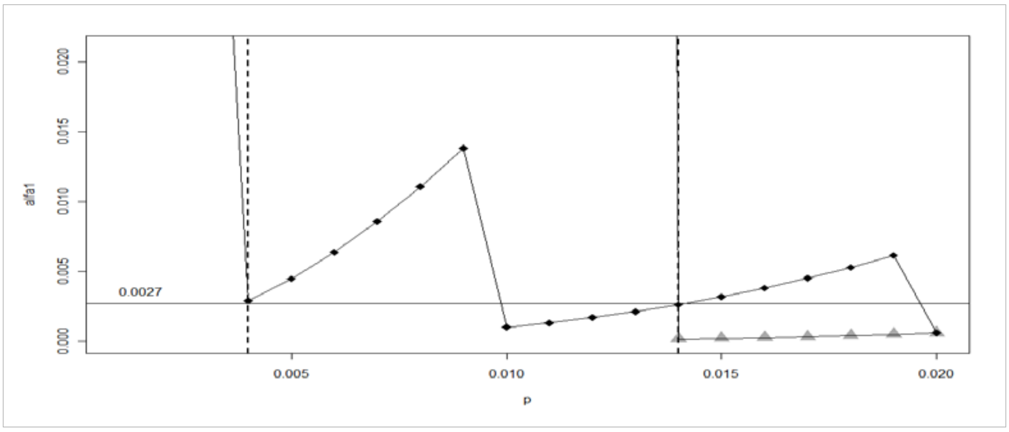

Figure 5: Alpha risk – Two sided (n = 20, p < 0.020)

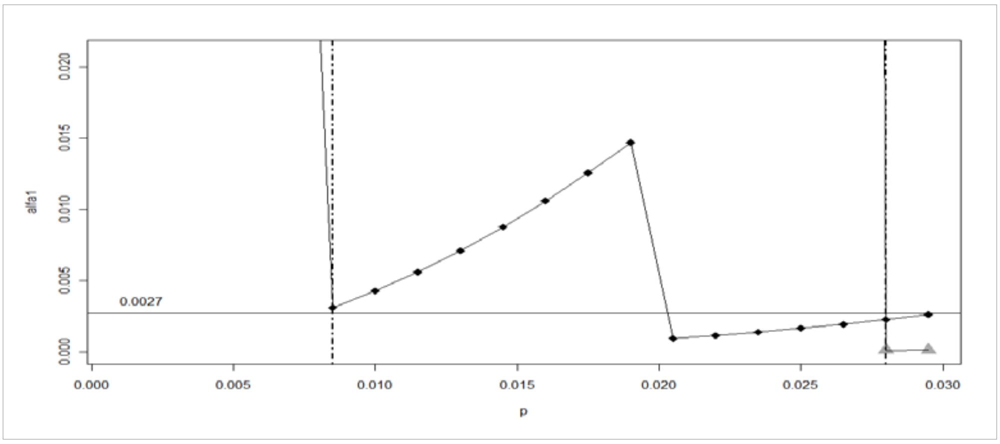

Figure 6: Alpha risk – Two sided (n = 10, p < 0.030)

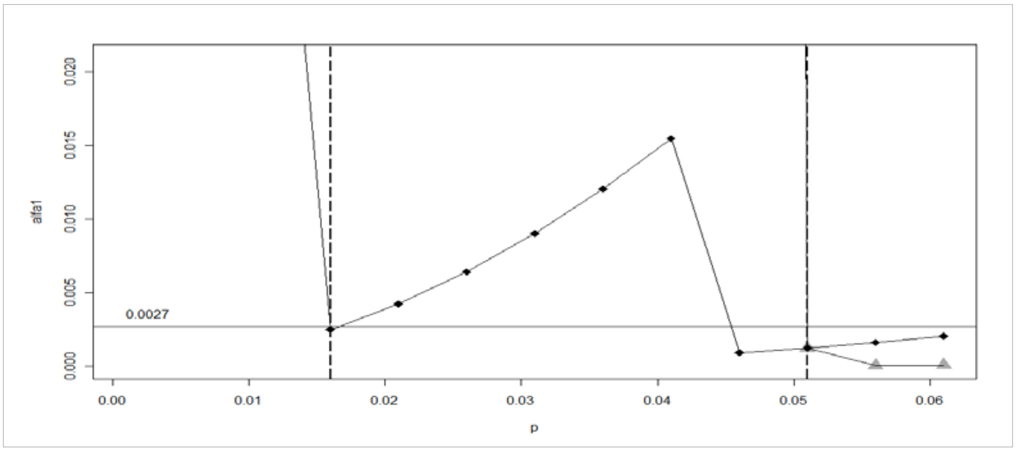

Figure 7: Alpha risk – Two sided (n = 5, p < 0.06)

From the figures above, we can see that, although the Cornish-Fisher correction with one term works well with small values of *p*, the one with two-terms shows better results, especially in the vicinity of zero (very high quality processes).

For example, for n = 20 (see Fig.5), we can use *p* charts with modified control limits with two correction terms when *p* is over 0.004, while with just one term of correction we can only use *p* charts when *p* is greater than 0.014 (more restrictive).

For n = 10 (see Fig. 6), the new modification allows working with values of *p* greater than 0.008, whereas previously we could work only with values of *p* greater than 0.028. When n = 5 (see Fig.7), we can now work with values of *p* over 0.016, whereas previously it was possible to work only with values of *p* over 0.051 (more restrictive).

In all cases, the excess of false alarm is substantially reduced.

Table 1 shows the minimum value of *p* possible to use in order to keep false alarm under control with: a) normal–based charts (without correction), b) Cornish-Fisher with one correction term (CF1), and c) Cornish-Fisher with two correction terms (CF2).

Table 1: Minimum values of p according to sample size and correction type

Sample size n	Minimum p			Minimum np			Minimum $np(1-p)$		
	Normal approx.	CF1	CF2	Normal approx.	CF1	CF2	Normal approx.	CF1	CF2
3	-	-	0.028	-	-	0.084			0.082
5	-	0.051	0.016	-	0.255	0.080	-	0.242	0.079
10	0.410	0.028	0.008	4.100	0.280	0.080	2.419	0.272	0.079
15	0.385	0.019	0.006	5.775	0.285	0.090	3.552	0.280	0.090
20	0.360	0.014	0.004	7.200	0.280	0.080	4.608	0.276	0.080
30	0.280	0.010	0.003	8.400	0.300	0.090	6.048	0.297	0.090
40	0.240	0.008	0.002	9.600	0.320	0.080	7.296	0.317	0.080
60	0.210	0.005	0.0013	12.600	0.300	0.078	9.954	0.299	0.078
100	0.150	0.003	0.0008	15.000	0.300	0.080	12.750	0.299	0.080

Minimum values of p were obtained considering the smaller value of p for which the α risk exists (finite) and is near the pre-fixed $\alpha = 0.0027$.

In general, there is agreement among several authors that when $np\ (1-p)$ is equal or greater than 5, and when p is greater than 0.10, it is appropriate to use the normal approximation to calculate the p chart limits (as we stated in Section 2.2 (*i*)). Based on the previous results, we see that it is possible to extend this rule to other values of n and p. In fact, we see that when $np\ (1-p) \geq 0.08$ we can consider the CF2 correction to calculate the control chart limits. When this calculation gives a value greater than 0.25, we can use either CF1 or CF2 to modify the control limits.

5. Numerical Illustration with Real Data

We shown one example illustrating the comparative performance of the three charts (Shewhart, one-term corrected and two-terms corrected) considering a process that produces chocolates (bonbons). For monitoring quality, a sample of 20 units is taken per hour of production and the numbers of chocolates with nonconformities in the envelopment are registered. A bonbon is nonconforming if it has one or more of the following characteristics:

• The chocolate is not whole, i.e. it has been crushed during the wrapping process
• Wrap has involved the chocolate only partially (i.e. chocolate is incomplete)
• The double twisted ribbons are not closed and well-armed

In order to illustrate the real possibility of false alarm (at the pre-fixed α_0 value) not by chance only but by the non-exactness of the normal approximated Shewhart limits, we present two control charts for the bonbons example with two-sided limits with sample size n = 20 and $\alpha_0 = 0.0027$.

In the first chart (Figure 8), we have compared the tree methodological possibilities considered in this paper (normal-based; CF1 and CF2). The vertical line indicate the separation of phase I (100 calibration samples used in the estimation of p), and phase II, where the new sample values are confronted through the statistic $\hat{p}$ with the control limits. The sample proportion of nonconforming estimated en phase I was $\hat{p} = 0.015$.

Figure 8: p Control Chart – Two sided, n = 20, $\hat{p}$ =0,015, $\alpha_0 = 0{,}0027$

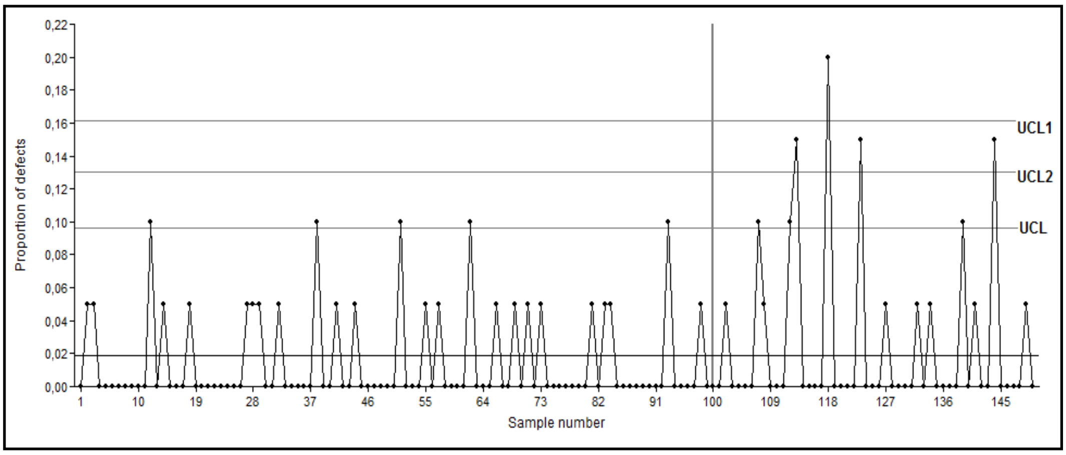

In this case, the control limits and α risk for the three charts (normal-based, CF1 and CF2) are as in Table 2 bellow. We considered only the upper control limit because the lower is close to zero or negative.

Table 2: Control limits and α risk from graphic of Figure 8

Type of chart	UCL	nUCL	α risk
Normal-approx.	0.0965	1.931	0.035746
CF1	0.1612	3.224	0.000202
CF2	0.1303	2.606	0.003178

Alwan (2000) pointed out that when using a symmetric distribution (normal) to approximate a skew binomial distribution (due the small values of p), it is possible that the lower control limit computed takes a negative value. In such cases, LCL is set equal to zero which implies, for all practical purposes, that the limit plays no role. When LCL equal zero, it is difficult to know if the subgroup proportion ($\hat{p}$) which is equal to zero reflects a true special cause or simply occurred because the true value of p is small. In our case, because p values are too small, the lower control limit will always be equal to 0. For practical purposes, the improvement of a process is determined by the estimated value of p monitored over the time.

In Figure 8 above, it is clear that the most appropriate limit is the one corresponding to CF2 (UCL2) because the normal-based (UCL) shows hypothetical false alarm signals and the limit based on CF1 has a lower probability of false alarm risk but it is far away from 0.0027.

Even though the process is in a state of statistical control, the proportion of nonconforming items was viewed as unacceptably high, and thus attention was directed to analyzing the system for improvement. Using problem-solving tools, the company manages to reduce the proportion of nonconforming bonbons to a value of $\hat{p}$ = 0.004. Figure 9 below, shows the control chart for this new hypothetical situation.

Figure 9: p Control Chart – Two sided, n = 20, $\hat{p}$ =0,004, $\alpha_0 = 0.0027$

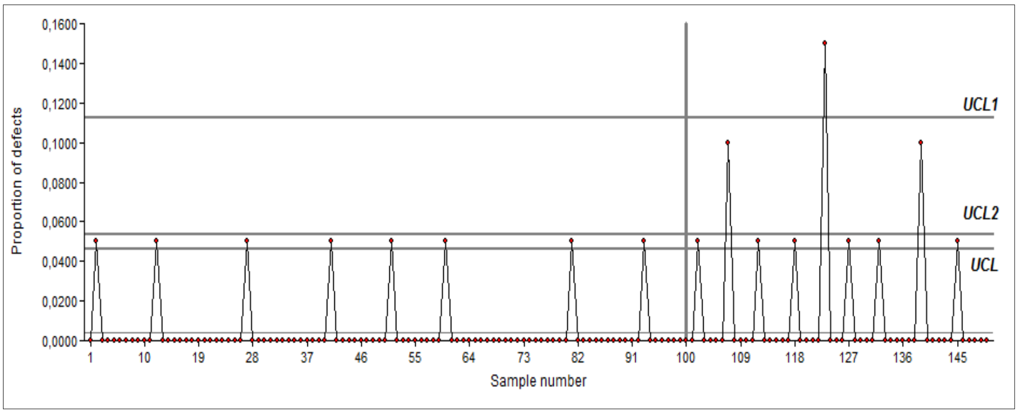

The control limits and α risk for the three charts (normal-based, CF1 and CF2) are as shown in Table 4. Again, we considered only the upper control limit because the lower is close to zero or negative.

Table 4: Control limits and α risk form graphic of Figure 8

Type of chart	UCL	nUCL	α risk
Normal-approx.	0.0463	0,926	0.077032
CF1	0.1125	2,250	0.923038
CF2	0.0533	1,066	0.002898

In this situation, the normal-based control limits show permanent signs of false alarm (because the upper control limit UCL is inappropriate). Also, it is not suitable for process control since the presence of only one nonconformity indicates a state of out of control. The CF1correction is also inadequate because it shows a very high risk of false alarm. This is shown in Fig. 5 where $\hat{p}$ =0.004 does not appear, because it hasn´t α risk in the neighborhood of 0.0027. Note that in this case, *np* (1-*p*) is equal to 0.08, which is the lowest value suggested to use the CF2 correction in the control limits (see Table 1).

6. Final Comments and Conclusions

In high quality processes usually the values of *p* are very small and the sample sizes are not large enough. This situation determines that conventional Shewhart *p* charts have serious drawbacks in detecting nonconforming products. The Cornish-Fisher expansion can directly determine adjustments on the control limits that improve probabilistic properties of *p* charts, in terms of putting false alarm risk under control.

In this paper we show a correction in *p* chart based on the Cornish-Fisher quantile correction formula by including terms of order $n^{-3/2}$. Just including 4^{th} order cumulants, this modified *p* chart has some advantages especially in the sense that it allows monitoring lower values of *p*, as is the case of very high quality processes.

At the same time, the gain in terms of practically eliminating the false alarm drawback of the traditional *p* chart is significant.

In addition, we suggest a new rule to consider the choice of the appropriate *p* chart. Without correction, with one term of correction and with two terms of correction, as follow:

When *np* (1-*p*) ≥ 5 without correction
When *np* (1-*p*) ≥ 0.25 one term of correction

When $np\,(1-p) \geq 0.08$ two terms of correction

Finally we expect that the QC practitioner can now use *p* chart for monitoring very high quality processes. The advantage associated with this simple adjustment is that user can insert this control limits in a statistical software in a very easy form.

References

[1] Acosta-Mejia, C. A. (1999). "Improved p charts to monitor process quality". IIE Transactions, vol. 31, pp 509-516.

[2] Alwan, L. C. (2000). *Statistical Process Analysis*. Mc Graw-Hill

[3] Chan, L.Y., Lin, D.K.J., Xie, M. and Goh, T.N., (2002), "Cumulative probability control charts for geometric and exponential process characteristics", *International Journal of Production Research* 38, 2, pp. 397-408

[4] Chen, G. (1998). "An improved p chart through simple adjustment". *Journal of Quality Technology*, 30, pp 142-151.

[5] Cornish, E.A. and Fisher, R.A. (1960). "The Percentage Points of distributions Having Know Cumulants". *Technometrics* 2, pp. 209-225.

[6] DeVor, R. E., Chang, T. and Sutherland, J. W. (2007) . *Statistical Quality Design and Control*, 2nd edition, Pearson / Prentice-Hall.

[7] Ermer, D.S. (1995), "Advanced SPC for high quality electronic card manufacturing", *Quality Engineer* 8, pp. 283–299.

[8] Goh T.N. and Xie M., (1995). "Statistical process control for low nonconformity processes", *International Journal of Reliability, Quality and Safety Engineering*, 2 pp. 15–22.

[9] Kuralmani V., Xie M., Goh T.N. and Gan F.F., (2002). "A conditional decision procedure for high yield processes", *IIE Transaction*, 34, pp. 1021–1030.

[10] Lee, Y. and Lee, M:C: (1992). "On the derivation and Computation of the Cornish-Fisher Expansion". *Australian Journal of Statistic*. 34, 3, pp.443-450.

[11] Lee, Y. S. and Lin, T. K. (1992). "Algorithm AS269: Higher-Order Cornish-Fisher Expansion". *JRSS Series C Applied Statistics*, 41, 1, pp 233-240.

[12] Montgomery, D .C. (2008). *Introduction to Statistical Quality Control*. 6th ed., Wiley

[13] Quesenberry C.P., (1997). *SPC Methods for Quality Improvement*, Wiley, New York.

[14] Recchia, D. & Barbosa, E. P.(2009) . "IQCC: An R Package for Improved Quality Control Charts". Available from CRAN.

[15] Ryan T.P., and Schwertman, N.C, (1997). "Optimal limits for attributes control charts" *Journal of Quality Technology***,** 29, pp. 86–98.

[16] Shewhart, W.A. (1926). "Quality Control Charts. Bell System" *Technical Journal* 5, pp. 593-603.

[17] Wang, H. (2009). "Comparison of p control charts for low defective rate" *Computational Statistics and Data Analysis*. 53, 12, pp 4210-4220.

[18] Winterbottom, A. (1993). "Simple adjustments to improve control limits on attribute charts". *Quality and Reliability Engineering International*, 9, 2, pp 105-109.

[19] Wu Z., Yeo S.H. and Fan H.T., (2000). "A comparative study of the CRL-type control charts" *Quality and Reliability Engineering International* 16, pp. 269–279.

[20] Xie M. and Goh T.N., (1993)." Improvement detection by control charts for high yield processes" *International Journal of Quality and Reliability Management* 10, pp. 24–31.

[21] Xie, M.; Goh, T. N. and Kuralmani,V. (2002). *Statistical Models and Control Charts for High Quality Processes*. Kluwer Academic Publ.